

Synthesis and Structural Study of a Novel Mixed Phosphate: $\text{Cd}_{0.5}\text{Zn}_{2.5}(\text{PO}_4)_2 \cdot 4\text{H}_2\text{O}$

Khalil Ahraifou, Jamal Khmiyas*, Mohammed Hadouchi, Abderrazzak Assani, Mohamed Saadi and Lahcen El Ammari

Laboratoire de Chimie Appliquée des Matériaux, Centre des Sciences des Matériaux, Faculty of Science, Mohammed V University in Rabat, Avenue Ibn Battouta, BP 1014, Rabat, Morocco

*Correspondence to:

Jamal Khmiyas
Laboratoire de Chimie Appliquée des Matériaux,
Centre des Sciences des Matériaux,
Faculty of Science,
Mohammed V University in Rabat,
Avenue Ibn Battouta,
BP 1014, Rabat, Morocco.
E-mail: j.khmiyas@um5r.ac.ma

Received: July 25, 2023

Accepted: September 26, 2023

Published: September 29, 2023

Citation: Ahraifou K, Khmiyas J, Hadouchi M, Assani A, Saadi M, et al. 2023. Synthesis and Structural Study of a Novel Mixed Phosphate: $\text{Cd}_{0.5}\text{Zn}_{2.5}(\text{PO}_4)_2 \cdot 4\text{H}_2\text{O}$. *NanoWorld J* 9(S2): S367-S371.

Copyright: © 2023 Ahraifou et al. This is an Open Access article distributed under the terms of the Creative Commons Attribution 4.0 International License (CCBY) (<http://creativecommons.org/licenses/by/4.0/>) which permits commercial use, including reproduction, adaptation, and distribution of the article provided the original author and source are credited.

Published by United Scientific Group

Abstract

Single crystals of the new phosphate $\text{Cd}_{0.5}\text{Zn}_{2.5}(\text{PO}_4)_2 \cdot 4\text{H}_2\text{O}$ were successfully grown hydrothermally and structurally determined by single crystal X-ray diffraction data. This new phase is isotypic with the Hopeite and crystallizes in the orthorhombic space group *Pnma* with the cell parameters $a = 10.6592(9) \text{ \AA}$, $b = 18.408(2) \text{ \AA}$ and $c = 5.0565(4) \text{ \AA}$. This crystal structure contains seven independent fully occupied cationic sites. The first six, that is located in 4c (.m.) Wyckoff positions, accommodate Cd(1)/Zn(1), four sites are filled by Zn(2) and three hydrogen, while the remaining site is entirely occupied by one P atom. This crystal structure can be described in terms of a net framework built up from a slightly distorted $(\text{Cd}(1)/\text{Zn}(1))\text{O}_2(\text{OH})_4$ octahedra and regular $\text{Zn}(2)\text{O}_4/\text{PO}_4$ tetrahedra units. In the structure, two $\text{Zn}_2(2)\text{O}_7$ dimers are held together by means of PO_4 groups in such way to form zigzag chains of corner-sharing. Adjacent chains are connected with the apical corners resulting in a complex layer of three- and four-membered sequential rings extending along [001]. The stacked layers are bridged by $(\text{Cd}(1)/\text{Zn}(1))\text{O}_2(\text{OH})_4$ octahedra that stabilizes the structure.

Keywords

Hydrothermal synthesis, X-ray diffraction, Phosphate, Crystal structure

Introduction

Over the past decades, several transition metal phosphates have been widely synthesized and structurally investigated [1]. Among these phases are those with open structures that offer a considerable number of interesting geometries resulting in valuable physical properties [2]. In such compounds, the presence of orthophosphate groups stabilizes various cationic oxidation states and coordination numbers, providing a high level of stability for the anionic building units [3]. Furthermore, due to their flexibility, these structures allow a wide range of metal substitutions leading to outstanding behaviors. For instance, gradually increasing of Metal/P ratio leads to denser and more rigid structures (e.g., CAS, ABW, BIK, and ANA zeotypes families) [4] and improves the capacity, lifetime, and throughput capability of $\text{Li}_{0.98}\text{Al}_{0.02}\text{FePO}_4/\text{C}$ mixed cathode [5]. In addition, one interesting approach for developing new nonlinear optical materials is the inclusion of specific d^{10} transition metal cations, such as Zn^{2+} and Cd^{2+} , that are sensitive to high polarization into metal phosphate matrix. These ions can also exhibit a number of coordination polyhedra, like ZnO_n ($n = 4, 5, \text{ and } 6$) and CdO_m ($m = 6, 7, \text{ and } 8$), that will offer options for predicting and designing new open frameworks. Net frameworks comprising interstitial voids are of considerable interest particularly in phosphate-based divalent cations, due to their promising applications in different fields such oxygen electrocatalysis [7], luminescence [8], anticorrosive pigments [9], biomedical sector [10], ceramics [11], lithium-ion

batteries [12], and automotive industry [13]. In the course of our research, we were able to synthesize and structurally characterize several hydrated phosphates based on transition metals, namely $Co_{2.39}Cu_{0.61}(PO_4)_2 \cdot H_2O$ [14], $Co_2Pb(HPO_4)(PO_4)OH \cdot H_2O$ [15], $Mn_2Zn(PO_4)_2 \cdot H_2O$ [16], $Ni_2Sr(PO_4)_2 \cdot 2H_2O$ [17] and $Mg_{1-x}Cu_x(PO_4)_2 \cdot H_2O$ where ($x = 1.26$ [18] or 1.35 [19]). The present paper reports the hydrothermal synthesis and structural study using single-crystal X-ray diffraction of the novel phosphate $Cd_{0.5}Zn_{2.5}(PO_4)_2 \cdot 4H_2O$ belonging to the Hopeite family.

Experimentation

Single crystals of $Cd_{0.5}Zn_{2.5}(PO_4)_2 \cdot 4H_2O$ were provided hydrothermally using an optimal reaction mixture of $Cd(NO_3)_2 \cdot 4H_2O$, ZnO , and H_3PO_4 (85% by weight), adjusted in agreement with the molar ratios of $Cd:Zn:P = 1:3:3$. The hydrothermal process was carried out over two days at 473 K in a suitable autoclave reactor using a 23 ml PTFE-lined container that was only halfway filled with deionized water. The reaction mixture was filtered, washed with distillate water, and air dried at room temperature. The colorless crystals obtained in parallelepiped shape correspond to this newly formed phase. The structure is determined at nanometric scale.

Results and Discussion

Structure determination

To collect X-ray diffraction data, a proper single crystal was picked using a polarizing microscope and mounted on a Bruker X8 APEX-II diffractometer. The observed data were gathered at 296 K utilizing the X-ray $MoK\alpha$ radiation ($\lambda = 0.71073 \text{ \AA}$) and the φ - ω scanning procedure on the whole sphere of reciprocal space. Integration, scaling, filtering, reflections merging, and correction of Lorentz-polarisation effects were carried out with the SAINT program [20]. Supplementary empirical absorption corrections using the SADABS program were also undertaken [21]. At this stage a total of 13878 intensities, of which 2418 are independent and 2049 meets the $I > 2(I)$ condition were obtained successfully. The structural elucidation of the title phosphate was carried out using the WinGX suite [22]. The current crystal structure was solved by Direct Methods with the SHELXT 2014/7 program [23] and then refined by SHELXL2018/3 program [24]. As a result of the structural resolution the Zn, Co, and P atoms were located first in the asymmetric unit, while the remaining oxygen and hydrogen atoms were positioned after numerous repetitive refinements and Fourier-difference analysis. During the refinement, hydrogen atoms were introduced in a riding model, with $U_{iso}(H)$ fixed at $1.5 U_{iso}(O)$ and O-H bond length limited to 0.82 \AA . The anisotropic and isotropic refinements carried out on the H and non-hydrogen atom coordinates, respectively lead to the given structural model. The last refining cycle yields the following residual electron densities $\Delta\rho_{min} = -0.81 \text{ e.\AA}^{-3}$ at 0.41 \AA from H7B and $\Delta\rho_{max} = 0.72 \text{ e.\AA}^{-3}$ at 0.65 \AA from Zn1. Table 1 contains the crystal characteristics, data collection, and structural refinement results.

Atomic positions and their corresponding displacement parameters are reported in table 2 and table 3. The number

Table 1: Crystal details, X-ray data collecting, and structural refinement results for $Cd_{0.5}Zn_{2.5}(PO_4)_2 \cdot 4H_2O$.

Crystal details	
Chemical formula	$Cd_{0.5}Zn_{2.5}(PO_4)_2 \cdot 4H_2O$
M_r	481.63
System, space group	Orthorhombic, $Pnma$
T (K)	296
a, b, c (\AA)	10.6592 (9), 18.408 (2), 5.0565 (4)
V (\AA^3)	992.2 (2)
Z	4
Mo $K\alpha$	$\lambda = 0.71073 \text{ \AA}$
μ (mm^{-1})	7.44
Data acquisition	
$\theta_{min}, \theta_{max}$ ($^\circ$)	3.8, 36.2
Miller indices	$-16 \leq h \leq 17, -29 \leq k \leq 29, -8 \leq l \leq 8$
Measured reflections	13878
Independent reflections	2418
Reflections with $I > 2\sigma(I)$	2049
R_{int}	0.037
$(\sin \theta/\lambda)_{max}$ (\AA^{-1})	0.832
Refinement	
$R[F^2 > 2s(F^2)], wR(F^2), S$	0.024, 0.056, 1.06
Number of variables	82
$\Delta\rho_{max/min}$ (e.\AA^{-3})	0.72, -0.81

of inter-atomic bond lengths and bond valence sum (BVS) are given in table 4 and the number characteristics of the hydrogen bond are given in table 5. Structural representations were done using Vesta-3 [25] and Ortep-3 [26].

Crystal structure description

This new phosphate's crystal structure may be defined as a net framework made up of significantly deformed $(Cd(1)/Zn(1))O_2(H_2O)_4$ octahedra and two regular $Zn(2)O_4$ and $P(1)O_4$ tetrahedra (Figure 1).

In the structure, $Zn(2)O_4$ units are held together by means of the connecting PO_4 groups in a manner as to create zigzag chains of corner-sharing. Adjacent chains are connected with

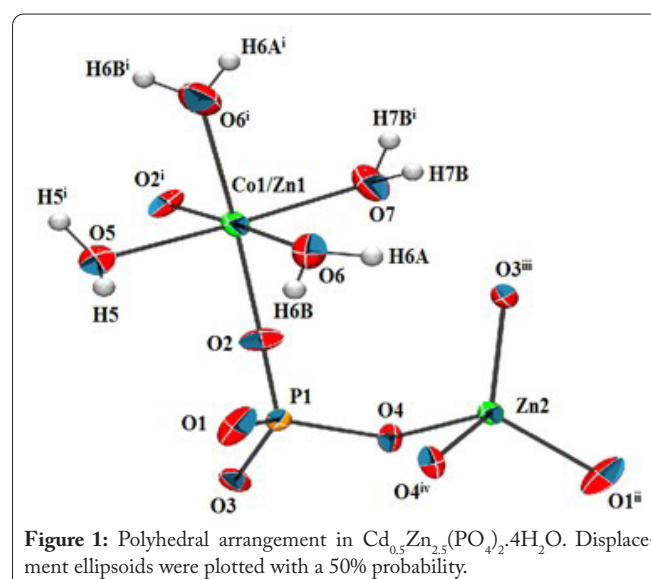


Figure 1: Polyhedral arrangement in $Cd_{0.5}Zn_{2.5}(PO_4)_2 \cdot 4H_2O$. Displacement ellipsoids were plotted with a 50% probability.

Table 2: Atomic positions and isotropic or equivalent thermal parameters (\AA^2) in $Cd_{0.5}Zn_{2.5}(PO_4)_2 \cdot 4H_2O$.

Atom	Site	x	y	z	U_{iso}^*/U_{eq}	Occ. (<1)
Cd1	4c	0.74199 (2)	0.250000	0.06018 (4)	0.01788 (5)	0.5
Zn1	4c	0.74199 (2)	0.250000	0.06018 (4)	0.01788 (5)	0.5
Zn2	8d	0.85628 (2)	0.49930 (2)	0.20851 (4)	0.01380 (5)	
P1	8d	0.60241 (4)	0.40739 (2)	0.22589 (8)	0.01312 (8)	
O1	8d	0.6005 (2)	0.42161 (8)	-0.0695 (2)	0.0300 (3)	
O2	8d	0.6391 (2)	0.32968 (8)	0.2856 (3)	0.0241 (3)	
O3	8d	0.4749 (2)	0.42295 (7)	0.3548 (3)	0.0223 (3)	
O4	8d	0.6973 (2)	0.46105 (7)	0.3593 (2)	0.0176 (2)	
O5	4c	0.6055 (2)	0.250000	-0.2601 (4)	0.0239 (4)	
H5	8d	0.609538	0.285875	-0.355887	0.036*	
O6	8d	0.8416 (2)	0.33439 (9)	-0.1831 (4)	0.0350 (4)	
H6A	8d	0.895348	0.359095	-0.109756	0.053*	
H6B	8d	0.808139	0.366201	-0.272047	0.053*	
O7	4c	0.8929 (2)	0.250000	0.3517 (5)	0.0349 (5)	
H7B	8d	0.957906	0.268204	0.295741	0.052*	

Table 3: Atomic displacement parameters (\AA^2) in $Cd_{0.5}Zn_{2.5}(PO_4)_2 \cdot 4H_2O$.

Atom	U^{11}	U^{22}	U^{33}	U^{12}	U^{13}	U^{23}
Cd1	0.01534 (9)	0.0228 (2)	0.01555 (9)	0.000	0.00001 (7)	0.000
Zn1	0.01534 (9)	0.0228 (2)	0.01555 (9)	0.000	0.00001 (7)	0.000
Zn2	0.01250 (9)	0.0179 (2)	0.01104 (8)	-0.00018 (6)	-0.00029 (6)	-0.00093 (6)
P1	0.0162 (2)	0.0121 (2)	0.0112 (2)	-0.0013 (2)	-0.0002 (2)	0.0016 (2)
O1	0.058 (2)	0.0208 (7)	0.0118 (5)	-0.0113 (6)	-0.0064 (6)	0.0036 (4)
O2	0.0354 (7)	0.0158 (6)	0.0210 (6)	0.0068 (5)	0.0085 (5)	0.0049 (4)
O3	0.0128 (5)	0.0193 (6)	0.0346 (7)	0.0003 (4)	0.0016 (5)	0.0066 (5)
O4	0.0144 (5)	0.0244 (6)	0.0139 (5)	-0.0052 (4)	0.0023 (4)	-0.0039 (4)
O5	0.0258 (9)	0.025 (1)	0.0210 (9)	0.000	0.0022 (7)	0.000
O6	0.0274 (7)	0.0320 (8)	0.046 (2)	-0.0047 (6)	-0.0041 (7)	-0.0077 (7)
O7	0.0208 (9)	0.054 (2)	0.03 (2)	0.000	0.0003 (8)	0.000

Table 4: Selection of bond lengths and cationic bond valence sum in the crystal structure of $Cd_{0.5}Zn_{2.5}(PO_4)_2 \cdot 4H_2O$.

Bond	Length (\AA)	Bond	Length (\AA)
Cd1/Zn1—O2	2.157 (2)	Zn2—O4	1.987 (2)
Cd1/Zn1—O2	2.157(2)	Zn2—O4	1.994 (2)
Cd1/Zn1—O5	2.177 (2)	$\langle \text{Zn2—O} \rangle = 1.9484 \text{ \AA}$	
Cd1/Zn1—O7	2.182 (2)	BVS(Zn2) = 2.08 v.u	
Cd1/Zn1—O6	2.248 (2)	P1—O2	1.514 (2)
Cd1/Zn1—O6	2.248 (2)	P1—O1	1.516 (2)
$\langle \text{Cd1/Zn1—O} \rangle = 2.1948 \text{ \AA}$		P1—O3	1.535 (2)
BVS(Cd1/Zn1) = 2.17 v.u		P1—O4	1.567 (2)
Zn2—O1	1.895 (2)	$\langle \text{P1—O} \rangle = 1.5329 \text{ \AA}$	
Zn2—O3	1.917 (2)	BVS(P1) = 5.02 v.u	

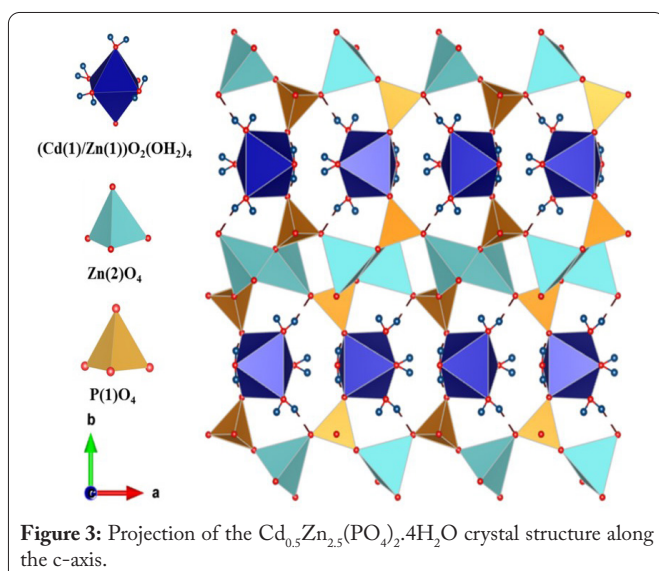
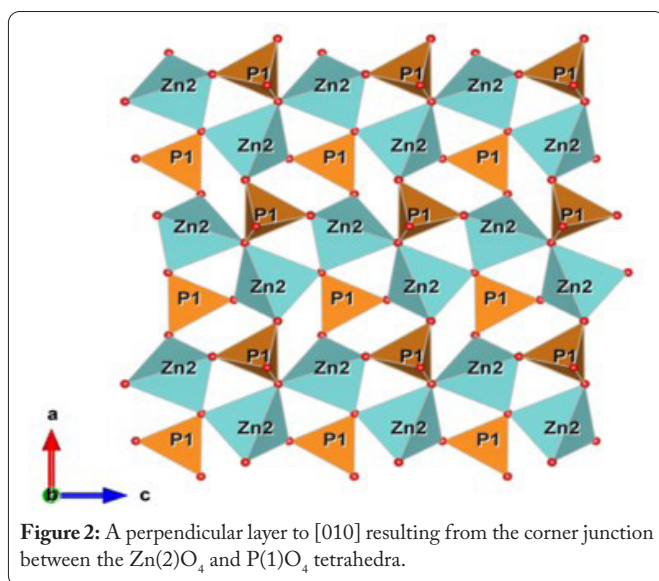
the apical corners resulting in a complex layer of three- and four-membered sequential rings running parallel to [001] (Figure 2). The stacked layers are bridged by (Cd(1)/Zn(1)) $O_2(OH_2)_4$ octahedra that stabilizes the structure by means of two oxygen atoms positioned in cis- configuration. The existence of water molecules in the resulting interstitial space also enhances cohesiveness between the neighboring layers through the hydrogen bonds (Figure 3).

Table 5: Hydrogen-bonding geometry in $Cd_{0.5}Zn_{2.5}(PO_4)_2 \cdot 4H_2O$ crystal structure.

$D-H \cdots A$ ($^\circ$)	$D-H$ (\AA)	$H \cdots A$ (\AA)	$D \cdots A$ (\AA)	$D-H \cdots A$ ($^\circ$)
O5—H5 \cdots O1	0.82	2.89	3.3033 (16)	114
O5—H5 \cdots O2	0.82	2.01	2.749 (2)	150
O5—H5 \cdots O3	0.82	3.25	3.9833 (17)	150
O6—H6A \cdots O1	0.82	2.96	3.429 (2)	119
O6—H6A \cdots O2	0.82	3.12	3.756 (2)	136
O6—H6A \cdots O3	0.82	1.94	2.726 (2)	160
O6—H6B \cdots O1	0.82	2.64	3.085 (2)	115
O6—H6B \cdots O2	0.82	2.95	3.447 (2)	121
O6—H6B \cdots O4	0.82	2.81	3.627 (2)	172
O6—H6B \cdots O4	0.82	3.25	3.794 (2)	127
O7—H7B \cdots O2	0.82	2.28	3.086 (2)	169
O7—H7B \cdots O2	0.82	2.67	3.086 (2)	113
O7—H7B \cdots O3	0.82	2.95	3.4623 (16)	122

Conclusion

Single crystals of $Cd_{0.5}Zn_{2.5}(PO_4)_2 \cdot 4H_2O$ were successfully obtained hydrothermally and their structure was established by single crystal X-ray diffraction analysis. This newly identified phase is isotypic with Hopeite and crystallizes in the orthorhombic space group Pnma with cell parameters



$a = 10.6592(9) \text{ \AA}$, $b = 18.408(2) \text{ \AA}$, and $c = 5.0565(4) \text{ \AA}$. The crystal structure of this phase is describable in terms of a net framework made up of slightly distorted $(Cd(1)/Zn(1))O_2(OH_2)_4$ octahedra and two regular $Zn(2)O_4/PO_4$ tetrahedra units. In the structure, $Zn(2)O_4$ groups are linked to each other by means of PO_4 units to form zigzag chains by corner-sharing. Neighboring chains are connected by apical corners, yielding a complex layer of three- and four-membered consecutive rings running along [001]. The Stacking layers are bounded by $(Cd(1)/Zn(1))O_2(OH_2)_4$ octahedra that stabilize the structure.

Acknowledgements

The authors are very grateful to the UATRS-CNRST, Rabat, Morocco for the X-ray analysis.

Conflict of Interest

None.

Funding

This project was funded by Mohammed V University, Rabat, Morocco.

References

- Rao CNR, Natarajan S, Neeraj S. 2000. Building open-framework metal phosphates from amine phosphates and a monomeric four-membered ring phosphate. *J Solid State Chem* 152(1): 302-321. <https://doi.org/10.1006/jssc.2000.8676>
- Morozov VA, Pokholok KV, Lazoryak BI, Malakho AP, Lachgar A, et al. 2003. A new iron oxophosphate $SrFe_3(PO_4)_3O$ with chain-like structure. *J Solid State Chem* 170(2): 411-417. [https://doi.org/10.1016/S0022-4596\(02\)00133-0](https://doi.org/10.1016/S0022-4596(02)00133-0)
- Natarajan S, Mandal S. 2008. Open-framework structures of transition-metal compounds. *Angew Chemie Int Ed* 47(26): 4798-4828. <https://doi.org/10.1002/anie.200701404>
- Henry PF, Kimber SA, Argyriou DN. 2010. Polymorphism and piezochromicity in the three-dimensional network-based phosphate $RbCuPO_4$. *Acta Cryst Sec B Struct Sci* 66(4): 412-421. <https://doi.org/10.1107/S0108768110020720>
- Xie H, Zhou Z. 2006. Physical and electrochemical properties of mixed-doped lithium iron phosphate as cathode material for lithium ion battery. *Electrochim Acta* 51(10): 2063-2067. <https://doi.org/10.1016/j.electacta.2005.07.014>
- Timofeeva MN, Panchenko VN, Hasan Z, Jhung SH. 2013. Catalytic potential of the wonderful chameleons: nickel phosphate molecular sieves. *Appl Catal A Gen* 455: 71-85. <https://doi.org/10.1016/j.apcata.2013.01.019>
- Zhan Y, Lu M, Yang S, Xu C, Liu Z, et al. 2016. Activity of transition-metal (manganese, iron, cobalt, and nickel) phosphates for oxygen electrocatalysis in alkaline solution. *Chem Cat Chem* 8(2): 372-379. <https://doi.org/10.1002/cctc.201500952>
- Ning Q, Quan B, Shi Y. 2019. Effect of alkali metal ions on the spectra of $CaZn_2(PO_4)_2 \cdot Sm^{3+}$ phosphor analyzed by JO theory. *J Lumin* 206: 498-508. <https://doi.org/10.1016/j.jlumin.2018.10.101>
- Ding S, Wang M. 2008. Studies on synthesis and mechanism of nano- $CaZn_2(PO_4)_2$ by chemical precipitation. *Dyes Pigm* 76(1): 94-96. <https://doi.org/10.1016/j.dyepig.2006.08.010>
- Herschke L, Lieberwirth I, Wegner G. 2006. Zinc phosphate as versatile material for potential biomedical applications Part II. *J Mater Sci Mater Med* 17: 95-104. <https://doi.org/10.1007/s10856-006-6333-3>
- Dean-Mo L, Brown JJ. 1993. Thermal expansion of porous $(Ca_{1-x}Mg_x)Zr_4(PO_4)_6$ ceramics. *Mater Chem Phys* 33(1-2): 43-49. [https://doi.org/10.1016/0254-0584\(93\)90088-4](https://doi.org/10.1016/0254-0584(93)90088-4)
- Deniard P, Dulac AM, Rocquefelte X, Grigorova V, Lebacqz O, et al. 2004. High potential positive materials for lithium-ion batteries: transition metal phosphates. *J Phys Chem Solids* 65(2-3): 229-233. <https://doi.org/10.1016/j.jpcs.2003.10.019>
- Parhi P, Manivannan V, Kohli S, McCurdy P. 2008. Room temperature metathetic synthesis and characterization of α -hopeite, $Zn_3(PO_4)_2 \cdot 4H_2O$. *Mater Res Bull* 43(7): 1836-1841. <https://doi.org/10.1016/j.materresbull.2007.07.005>
- Assani A, Saadi M, El Ammari L. 2010. Dicobalt copper bis[orthophosphate(V)] monohydrate, $Co_{2.39}Cu_{0.61}(PO_4)_2 \cdot H_2O$. *Acta Cryst E Cryst Commun* 66(5): i44. <https://doi.org/10.1107/S1600536810015382>
- Assani A, Saadi M, Zriouil M, El Ammari L. 2012. Dicobalt(II) lead(II) hydrogenphosphate(V) phosphate(V) hydroxide monohydrate. *Acta Cryst Sec E Cryst Commun* 68(5): i30. <https://doi.org/10.1107/S1600536812014870>
- Alhakmi G, Assani A, Saadi M, El Ammari L. 2015. Crystal structure of dimanganese(II) zinc bis[orthophosphate(V)] monohydrate. *Acta Cryst Sec E Cryst Commun* 71(2): 154-156. <https://doi.org/10.1107/S2056989015000341>

17. Assani A, Saadi M, Zriouil M, El Ammari L. 2010. $Ni_2Sr(PO_4)_2 \cdot 2H_2O$. *Acta Cryst Sec E Cryst Commun* 66(12): i86-i87. <https://doi.org/10.1107/S1600536810045113>
18. Khmiyas J, Assani A, Saadi M, El Ammari L. 2015. Crystal structure of magnesium copper(II) bis[orthophosphate(V)] monohydrate. *Acta Cryst Sec E Cryst Commun* 71(1): 55-57. <https://doi.org/10.1107/S2056989014026930>
19. Khmiyas J, Assani A, Saadi M, El Ammari L. 2022. Elaboration and characterization of a new phosphate $Mg_{1.74}Cu_{1.26}(PO_4)_2 \cdot H_2O$ with morphotropic structure. *Mater Today Proc* 58: 1069-1073. <https://doi.org/10.1016/j.matpr.2022.01.126>
20. Bruker SAINT-Plus. 2012. Bruker AXS Inc., Madison, Wisconsin, USA.
21. Krause L, Herbst-Irmer R, Sheldrick GM, Stalke D. 2015. Comparison of silver and molybdenum microfocus X-ray sources for single-crystal structure determination. *J Appl Cryst* 48(1): 3-10. <https://doi.org/10.1107/S1600576714022985>
22. Farrugia LJ. 2012. WinGX and ORTEP for Windows: an update. *J Appl Cryst* 45(4): 849-854. <https://doi.org/10.1107/S0021889812029111>
23. Sheldrick GM. 2015. SHELXT-Integrated space-group and crystal-structure determination. *Acta Cryst Sec A Found Adv* 71(1): 3-8. <https://doi.org/10.1107/S2053273314026370>
24. Sheldrick GM. 2015. Crystal structure refinement with SHELXL. *Acta Cryst Sec C Struct Chem* 71(1): 3-8. <https://doi.org/10.1107/S2053229614024218>
25. Momma K, Izumi F. 2011. VESTA 3 for three-dimensional visualization of crystal, volumetric and morphology data. *J Appl Cryst* 44(6): 1272-1276. <https://doi.org/10.1107/S0021889811038970>
26. Farrugia LJ. 1997. ORTEP-3 for Windows-a version of ORTEP-III with a Graphical User Interface (GUI). *J Appl Cryst* 30(5): 565. <https://doi.org/10.1107/S0021889897003117>